2009 IEEE International Conference on Robotics and Automation
Kobe International Conference Center
Kobe, Japan, May 12-17, 2009

A versatile wire robot concept as a haptic interface for sport simulation

Joachim v. Zitzewitz, Georg Rauter, Reto Steiner, Andreas Brunschweiler, and Robert Riener, *IEEE member*

***Abstract*— This paper presents the design of a new user-cooperative rope robot. This robot serves as a large-scale haptic interface in a multi-modal Cave environment used for sport simulation. In contrast to current rope robots, the configuration of the presented robot is adaptable to different simulation tasks what makes the robot more versatile. However, this adaptability and the high dynamics in sports lead to challenging requirements and specific design criteria of the hardware components. We present the requirements on the single robot components as well as the design of the entire setup optimized in terms of user-cooperativity and versatility. The setup includes sensors to measure the relevant parameters for user-cooperative control, i.e. position with a high resolution and the rope forces. Furthermore, an algorithm is introduced, which calculates the distance between the single ropes and the user in order to avoid collisions between the ropes and the user. Single points on the user's body are, therefore, tracked with a motion tracking system; the user's single body parts are then represented by geometrical objects whose distances to the ropes are calculated. The algorithm is programmed in such way that the collision detection runs in real-time. Both, the hardware and the algorithm, were evaluated experimentally in two applications, a rowing simulator and a tennis application. The hardware concept combined with the distance calculation allows the use of new kinematic concepts and expands the spectrum of realizable movement tasks that can be implemented into the Cave environment.**

I. Introduction

In recent years, an increasing effort has been put into the development and design of user-cooperative robots. These robots stay in direct contact with the human operator or are even attached to him. Thus, a careful selection of hardware components and control strategies is essential in order to guarantee user safety.

An interesting subgroup of user-cooperative robots are rope robots, also referred to as wire robots, cable robots, or tendon-based robots. In rope robots, the end-effector is supported in parallel by n cables. This support by cables is lightweight which improves the overall system dynamics. Additionally, this support provides general advantages of parallel-linked kinematic manipulators, such as high position accuracy and high rigidity. User-cooperative rope robots have already been implemented as rehabilitation devices [1], [2], [3], [4] and haptic interfaces in VR-environments [5], [6], [7], [8], [9], [10], [11], [12]. Most of these robots have a predefined configuration, i.e. the deflection points from which the ropes enter the workspace have got a fixed position. The fixed position of these deflection points limits the range of applications.

The goal of the project presented herein was the development of a large-scale (workspace: 4x6x5m), user-cooperative rope robot, called r^3 (Reactive Rope Robot). The system is planned to be used for research in motor learning with a special focus on sport simulations. In contrast to other systems, the configuration of the robot as well as the number of actuators are not fixed but can be adapted to each simulation task: for simple tasks such as 1D-contact problems, one or two ropes might be sufficient, while more complex, spatial tasks require the use of multiple ropes. Furthermore, a method was implemented to calculate the distance between the user and the rope. This method is not only a safety measure to prevent from a collision between the user and the rope. It also serves as a basis for more complex actuation and control concepts which increase the useable workspace and the number of implementable tasks. In combination with the adaptable robot configuration, this robot concept opens new fields of application for this robot type.

II. Hardware Setup

A. Overall setup: the r^3-system as a haptic display in a multi-modal Cave system

The r^3-system represents the haptic modality in a multi-modal Cave system, the so-called M^3-Lab (Fig. 1). The Cave

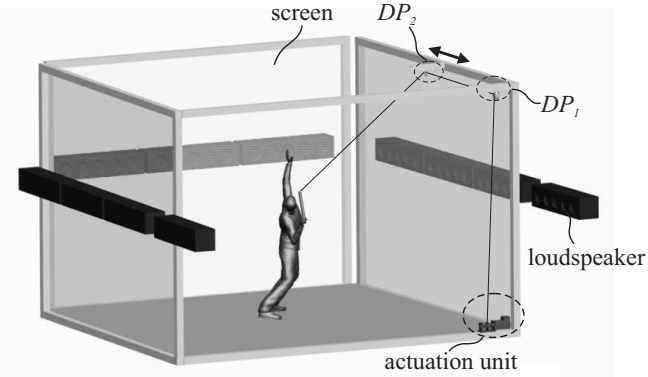

Fig. 1. The r^3-rope robot as a haptic display in the M^3-Lab (exemplarily, only one rope depicted); the position of the second deflection point (DP_2) can be adjusted along the Cave frame

J. von Zitzewitz is with Institute of Robotics and Intelligent Systems, ETH Zurich, 8092 Zurich, Switzerland zitzewitz@mavt.ethz.ch
G. Rauter is with Institute of Robotics and Intelligent Systems, ETH Zurich, 8092 Zurich, Switzerland rauter@mavt.ethz.ch
R. Steiner is with Institute of Robotics and Intelligent Systems, ETH Zurich, 8092 Zurich, Switzerland steinerr@ee.ethz.ch
A. Brunschweiler is with Institute of Robotics and Intelligent Systems, ETH Zurich, 8092 Zurich, Switzerland brunschweiler@mavt.ethz.ch
R. Riener is with Institute of Robotics and Intelligent Systems, ETH Zurich, 8092 Zurich, Switzerland and Spinal Cord Injury Center, University Hospital Balgrist, University of Zurich, 8008 Zurich, Switzerland riener@mavt.ethz.ch

TABLE I

DYNAMICS IN SPORTS

max. racket velocity (tennis) [13]	37.5 m/s
max. foot velocity (soccer) [14]	30 m/s
max. hand acceleration (general) [15]	27 m/s^2
max. hand force (rowing) [16]	800 N
continuous power (rowing) [16]	500-700 W
peak power (rowing) [16]	1000-1500 W

TABLE II

DYNAMIC PARAMETERS OF A SINGLE DRIVE TRAIN

max. velocity	18 m/s
peak force	1100 N
continuous force	300 N
power	1500 W

comprises also a 3D-projection on three screens and a sophisticated sound system (Iosono GmbH, Erfurt, Germany). Furthermore, a motion tracking system (QTM, Qualisys AB, Gothenburg, Sweden) is installed in the M^3-Lab.

The ropes of the r^3-systems are guided from the actuation unit (AU) over two deflection points (DP_1 and DP_2) into the workspace. The position of $DP1$ is fixed while the position of DP_2 is manually adjustable along the frame of the Cave in order to adapt the robot configuration to different tasks.

B. Actuation unit

In our application, several training scenarios for diverse sports should be implemented. Thus, the actuation should generate high velocities and accelerations as well as high power (Table I).

The entire drive train is designed to have minimal inertia and friction to warrant optimal performance in highly dynamic tasks. The actuation unit consists of three main parts: a motor, a safety brake, and a winch (Fig. 2).

1) Motor: The probably most common motor types in user-cooperative robotics are direct-current (DC) motors, which are integrated in many tendon-based systems [2], [3], [5], [10], [17], [18]. However, DC-motors are only available for a limited range of power. Thus, they do not fulfill the requirements presented above (Table I). Therefore, our choice fell on Danaher AC-brushless servo motors. A similar motor type has already been implemented in an other rope robot [30].

2) Safety brake: As a novel and important safety component, an electromagnetic safety brake (Robastop, Chr. Mayr GmbH + Co. KG, Mauerstetten, Germany) is mounted on the winch shaft coupled to the motor. This brake blocks the drive train in case of emergency or power breakdown. This safety measure is required when a sudden force decrease in case of a motor brake down could lead to injuries of the user. The brake can be permanently unblocked by fixing its hand release in order to prevent braking during the execution of dynamic movements. The state of the hand release is monitored with an integrated switch.

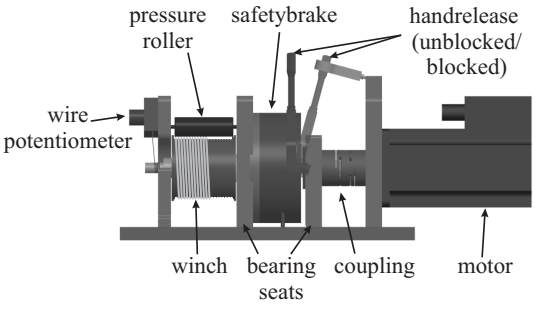

Fig. 2. Drive train of the r^3-system

3) Winch: The winch is directly coupled to the motor shaft in order to avoid gear friction. Instead of using a gear, the transmission of the actuation unit can be adapted by choosing the diameter d_W of the winch between 70-150 mm. In contrast to most rope robots, the winch is therefore not placed between the two bearing seats of the shaft but is mounted on the outer end of the shaft to enable a simple replacement for different tasks. The winch is made of ERTALON, a highly wear-resistant polyamide. A pressure roller prevents the rope from derailing.

This drive train configuration is optimized concerning friction and inertia. The inertia I_S of the entire shaft including the brake rotor and the largest winch is approximately four times higher than the inertia of the rotor of the motor I_M. Thus, the inertia I_O felt by the user on the drive side of the shaft is

$$I_O = I_S + I_M \approx 5 \cdot I_M. \tag{1}$$

The inertia of the shaft $I_{S_{min}}$ with the smallest winch mounted is $3.5 \cdot I_M$. In combination with a gear transmission of $u = 2$, this would lead to an inertia I_{Og} on the drive side of

$$I_{Og} = u^2 \cdot I_M + I_{S_{min}} \approx 7.5 \cdot I_M. \tag{2}$$

C. Ropes

The ropes represent the link between the actuator and the user. Thus, their choice is essential for both, the user safety and the system performance. Commonly used materials in rope robots are steel [2], [19], [20], [21], [22], [23] or different synthetic materials like Nylon [3], Armid [24], Kevlar [25], or Zylon [26]. The selection of the rope depends mainly on the following parameters: specific weight (kg/m), break load F_B (N), work stress (%), minimal bending radius r_{min} (m), tying, damping, and abrasion-resistance. In order to minimize the force error resulting from the oscillations of the rope, the rope should be lightweight and have low work strain. Furthermore, the risk of injury decreases with increasing stiffness of the ropes in the case of rope break, as stiff ropes store less potential energy. Note that knots or rope clips reduce the break load F_B considerably. To minimize this influence on F_B at the fixation point, the

TABLE III
ROPE PARAMETERS

material	Dyneema
diameter	4 mm
specific weight	$7 \cdot 10^{-3}$ kg/m
break load	12.5 kN
minimal bending radius	12 mm

fixation loop at the end of the rope should be realized by what is referred to as splicing. Splicing is a self-locking and non-destructive method to make loops at the end of a rope which minimizes the diminution of F_B at the fixation point. It is applicable to many synthetic ropes. The minimal bending radius r_{min} depends on the material and the rope diameter d_R: for steel wires, the minimal bending radius is $r_{min,steel} \approx 10 \ldots 12.5 d_R$; for synthetic ropes, the minimal bending radius is $r_{min,syn} \approx 2.5 \ldots 3 d_R$ [26]. Multiple tying of synthetic ropes provides positive effects on the bending radius but decreases the rope stiffness. Considering these criteria, we chose a synthetic rope made of Dyneema (Table III).

D. Deflection Units

The deflection units guide the rope from the actuation unit into the workspace. Their influence on the force transmission from the actuator to the end-effector has to be minimized. Thus, the deflection unit should have low inertia and low friction.

Some groups, e.g. [2], [24], [5], place the actuators of the robot at or near the deflection points where the ropes enter the workspace, most commonly at the corners of the robot frame. As in our case the positions of the deflection points change for different applications, the entire motor units ($\sim 13\,\mathrm{kg}$) would have to be re-mounted to adapt the robot configuration. Furthermore, the motor units should be easily accessible which is not the case for the upper part of the frame (5 m height). Thus, the actuators are installed at a fixed position at the lower edges of the Cave. Under this condition, at least two deflection points are needed for each rope to enter the workspace from any point of the frame.

The first deflection unit at DP_1 guides the rope from the winch to the second deflection point DP_2 (Fig. 1). It can be realized with a simple pulley as the angles between the pulley and the rope hardly change. The pulley is a custom-made product made of ERTALON with standard ball bearings. Alternative products proposed in the literature are sailing pulleys [27]. They have very low weight as the entire pulley including the balls of the bearings are made of plastic. They were not chosen for the r^3-system as test pulleys overheated and broke during pre-tests when turning with high speed under high load.

The second deflection unit at DP_2 guides the rope into the workspace. In some rope robots, the rope is guided through a small hole into the workspace [24], [25]. This solution facilitates kinematical calculation but leads to elevated friction and rope abrasion at the deflection point. A new deflection unit was designed which guides the rope via two pulleys and two rollers into the workspace (Fig. 3). Compared to swivel castors, this unit does not contain oscillating elements which could lead to lateral oscillation of the rope. Furthermore, the rope cannot derail and is guided through the narrow gap between screens with the deflection unit mounted behind the screen.

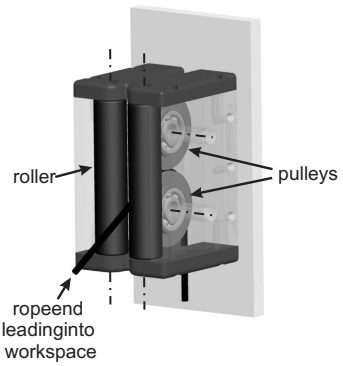

Fig. 3. Deflection unit at DP_2

E. Sensors

The choice of sensors influences the performance of the robot as well as the choice of implementable control concepts. In addition, the sensor concept is crucial with respect to the user's safety. We integrated sensors to measure position and force.

1) Position measurement: Like in most groups, the encoder attached to the motor is used for position measurement. The chosen motor comprises a 17-bit BISS-encoder. This results in a longitudinal resolution of 0.004 mm for the largest winch. This value is below the range of values we found for currently used devices (e.g. 0.025 mm [18], 0.038 mm [24]). Due to the high resolution, also the first and second derivatives have little noise. In addition, the absolute motor angle is measured with an analogue sensor. This redundant position measurement serves as a safety measure as it is often applied in user-cooperative devices [28], [29]. Furthermore, the analogue sensor makes the calibration of the robot axes dispensable because the absolute rope length is measured. We use a wire potentiometer wound around an axis at the outer end of the drive train (Fig. 2). With this setup, up to 20 revolutions can be measured. Furthermore, it does not get damaged if the motor overwinds: in one direction, the wire of the potentiometer runs off the axis; in the other direction, the fixation ring of the potentiometer jumps off its fixation hook (Fig. 4a).

2) Force measurement: Different solutions for the measurement of rope forces or man-machine interaction forces in rope robots have been applied. For instance, the forces are measured at the motor unit [30], [31] or directly at the end-effector [2]. However, many rope robots do not comprise any force/torque measurement devices: their force is only open-loop controlled as their actuators have a constant current-to-torque ratio. We decided to integrate force sensors in

our device for two reasons: firstly, more advanced user-cooperative control strategies (e.g. admittance control) can be implemented. And secondly, the integration of force sensors implies a significant increase of user safety. The force sensor is integrated into the deflection unit at DP_1, which guides the rope from the motor to the second deflection unit as the deflection angle around this pulley is constant. A similar solution is proposed by Fang [24]. The used sensors are one-roller tensionmeters (M1355, Tensometrics GmbH, Wuppertal, Germany) as they are implemented in coiling applications for tension control (Fig. 4b). The pulley at DP_1 is mounted on the axis of the tensionmeter. The systematic measurement error results from the interaction forces between the deflection unit at DP_2 and the rope.

III. Collision Detection between User and Ropes

In order to calculate the exact distance between the ropes of the robot and the user, the poses of the user's single body parts have to be known. Therefore, the user's movement was registered by the motion tracking system. Markers were placed on the shoulders, hip, head and arm joints as well as on the end-effector point. These points define the position of geometrical objects representing the user. The user is represented by polyhedrons formed by triangles (upper body) and cylinders with spherical cubs on both ends (head and arms) (Fig. 5).

There are several algorithms for collision detection and distance calculation available [32]. However, the problem of collision detection between a wire and arbitrary objects can be simplified by appropriate measures compared to the general collision detection problem between arbitrary objects. Therefore, we developed and implemented an algorithm optimized to the problem of collision detection in wire robots which is partially based on the existing algorithms [32], [33].

This algorithm was primarily developed to detect the collision between the ropes and the user as well as between different ropes (*auto-collision*). Furthermore, it is capable of identifying the object closest to each rope and the distance vector to this object.

The basic idea of the algorithm is to describe the geometrical objects in coordinate systems O_{R_i} $(i = 1..n)$ whose z-axes are aligned with the direction vectors of the n ropes. Due to this transformation, the problem can be broken down to a collision detection between the parallel projection of the

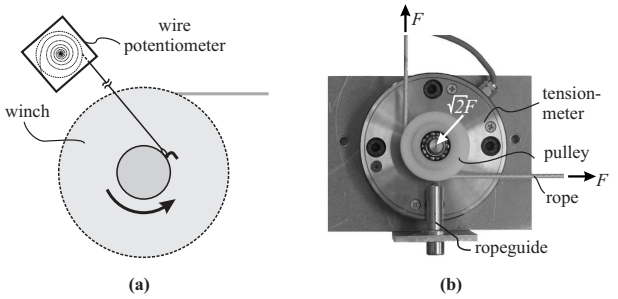

Fig. 4. a) Fixation of the wire potentiometer to the axis; b) One-roller tensionmeter for measurement of rope force

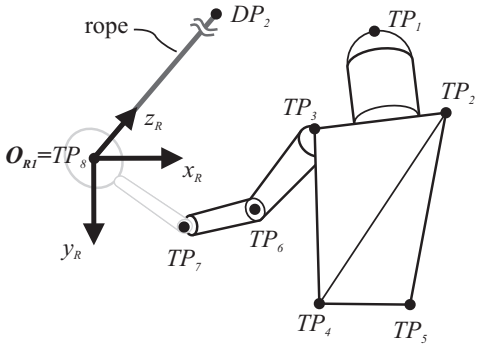

Fig. 5. Collision detection between one rope and the user: the user and the fixation point of the rope are tracked (tracking point $TP_i, i = 1 \ldots 8$)

geometrical objects on the xy-plane of O_{R_i} and a point (the origin of O_{R_i}) representing the rope (Fig. 5). The parallel projection of the chosen objects as well as the calculation of the distance between the projection and a point need little computation time. Hence, the collision detection can run in real-time with a sampling frequency of approximately 100 Hz even for multiple ropes and complex bodies. The proper collision detection without the distance calculation can run independently at a much higher sampling frequency.

IV. First Applications & Results

A. Robot Dynamics and Safety

At first view, the dynamics of the presented drive train do not fulfill the requirements for sport simulation (Table I, Table II), especially in terms of velocity. However, the end-effector velocity in specific workspace areas and directions can become more than three times larger than the velocity of a single axis depending on the robot configuration [27]. Thus, the required velocities can be reached by an appropriate choice of the configuration. In terms of actuator power, the motor is sufficiently dimensioned as it was already successfully implemented for the power-intensive task of rowing simulation (section IV-B).

The use of highly dynamic drive units connected directly or via an end-effector to the user requires high safety standards. For this purpose, the states of the robot are monitored by a state machine which defines three consecutive modes: In the first mode, the communication between the drives, the control PC, and the electronics is checked while the power supply of the motor drives is still disconnected. Subsequently, the state machine switches to a second mode during which the velocity and torque/force limits are set to small values (0.05 m/s and 50 N). From now on, the operator has to press a dead-man switch and keep it pressed during the entire operation. During the second state, the robot is pretensed and the function of all sensors is checked. After pretensioning the system, and the operator's confirmation on the graphical user interface, the state machine switches to the third mode, the actual operation mode. During this mode, the position, velocity and force/torque of all drive trains are continuously compared to their minimal and maximal admissible values which are task-dependent. Furthermore,

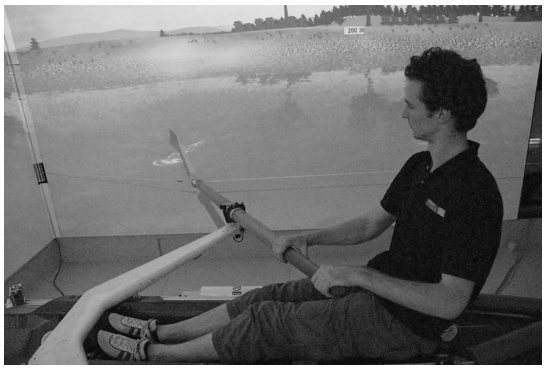

Fig. 6. Rowing simulator with multi-modal feedback in the M3-Lab

the communication with the drives and the sensor electronics are monitored. This safety concept was implemented and validated in two applications presented subsequently.

B. Rowing simulator

First, a rowing simulator was realized in the M^3-Lab. A hybrid active/passive actuation concept was implemented to render the hydrodynamical forces at the oar representing the end-effector (Fig. 6).The rowing model and on the setup are described in detail in [34]. In this application, high forces are applied under dynamic conditions by the robot. Thus, the development of the rowing simulator served as a good basis for tests of the endurance limit of the single components of the drive train. The components of the drive train presented herein were successfully used for an extensive study with ten novice and professional rowers.

C. Collision avoidance in virtual tennis

The algorithm for collision detection was validated with a simple setup (Fig. 7): one rope r_1 was connected to the end-effecter, a tennis racket, grasped by the user. The second rope r_2 was an elastic tendon (spring constant k) whose end was fixed; a third rope r_3 was connected to a drive train; The loose ends of all three ropes were connected together at the connection point P_C. This point was tracked together with the markers on the user's body described above (Fig. 5).

In this setup, variation of the motor torque τ lead to changes of the system pre-tension and, thus, to for- and backward movements of the deflection point P_C. For

$$\tau = \tau_{min}, \tag{3}$$

the point P_C moved to the front of the Cave (away from the actuation unit), while for the maximal pre-tension

$$\tau = \tau_{min} + \Delta\tau \tag{4}$$

it moved to the very back of the Cave.

The distance d between r_1 and the user was calculated as described in section III.

The motor torque τ was controlled in such way that a collision between r_1 and the user was avoided. Therefore, the following control law was applied as a function of the distance d:

$$\tau = \tau_{min} + \Delta\tau \cdot \frac{\tilde{d} - d_{min}}{d_{max} - d_{min}}. \tag{5}$$

with

$$\tilde{d} = \begin{cases} d_{max} & \text{for } d > d_{max} \\ d_{min} & \text{for } d < d_{min} \\ d & \text{otherwise} \end{cases} \tag{6}$$

This control law assured that the r_1 was always pulled away from the user. The test person could perform an entire forehand swing without colliding with the ropes. Furthermore, the controller also reacted when single body parts were approached towards the rope, i.e. the user could push away rope r_1 with the elbow or the head without touching it. The algorithm ran at 1 kHz.

V. Discussion and Conclusion

The aim of this project was the development of a versatile rope robot as a haptic interface for sport simulation. The presented hardware concept allows the choice of transmission within a certain range while reducing the friction and inertia of the robot compared to a system with gear transmission. This reduction of the system dynamics enhances the transparency of the robot, thus, reducing the distortion between the human-robot interaction force and the desired contact force. Overall, the drive train seems to fulfill the dynamical requirements for sport simulation. However, the actuation unit can easily be equipped with even stronger or faster motors; the chosen motor type is available in different velocity and power ranges and can be replaced without the need of adaptations of the electronics.

The knowledge of the distance between the user and the ropes opens new perspectives concerning actuation and control concepts. The presented application shows that already a simple control approach is sufficient to avoid the collision between the ropes of the robot and the user during the execution of complex body movements.

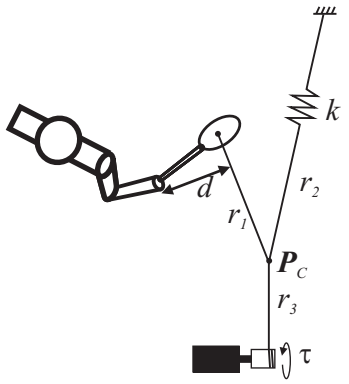

Fig. 7. Setup for the validation of the collision detection method: by increasing and decreasing the motor torque τ, the connection point P_C can be moved for- and backward. The torque τ is controlled as a function of the distance d between rope r_1 and the user

In summary, a robotic concept was presented which serves as a haptic display and is optimized for versatile use in sport simulation. In a next step, a methodology to calculate an optimal robot configuration for a given rendering task is developed.

REFERENCES

[1] K. Homma and T. Arai. Design of an upper limb motion assist system with parallelmechanism. In *Proc. IEEE International Conference on Robotics and Automation*, pages 1302–1307, 1995.

[2] D. Mayhew, B. Bachrach, W.Z. Rymer, and R.F. Beer. Development of the macarm - a novel cable robot for upper limb neurorehabilitation. In *Proc. 9th International Conference on Rehabilitation Robotics*, pages 299–302, June, July 2005.

[3] G. Rosati, P. Gallina, A. Rossi, and S. Masiero. Wire-based robots for upper-limb rehabilitation. *International Journal of Assistive Robotics and Mechatronics*, 7(2):3–10, 2006.

[4] D. Surdilovic and R. Bernhardt. String-man: a new wire robot for gait rehabilitation. In *Proc. IEEE International Conference on Robotics and Automation*, volume 2, pages 2031–2036, 2004.

[5] L. Bouguila, M. Ishii, and M. Sato. Scaleable spidar: A haptic interface for human-scale virtual environments. *Haptic Human-Computer Interaction*, 2058/2001:182–193, 2001.

[6] S. Hasegawa, M. Sato, Y. Dobashi, T. Yamamoto, M. Kato, and T. Nishita. Virtual canoe: real-time realistic water simulation for haptic interaction. In *Proc. International Conference on Computer Graphics and Interactive Techniques*, page 28, New York, NY, USA, 2005.

[7] M. Hirose, K. Hirota, T. Ogi, H. Yano, N. Kakehi, M. Saito, and M. Nakashige. Hapticgear: the development of a wearable force display system for immersive projection displays. In *Proc. IEEE Virtual Reality*, pages 123–129, Yokohama, Japan, March 2001.

[8] M. Ishii and M. Sato. A 3d interface device with force feedback: a virtual work space for pick-and-place tasks. In *Proc. IEEE Virtual Reality Annual International Symposium*, pages 331–335, Sept. 1993.

[9] S. Jeong, S. Shoichi Hasegawa, , and S. Sato Makoto. Haptic interaction toward co-evolutionary space. In *Proceedings of the Internatial Symposium on Ubiquitous VR 2006*, pages 21–24, Yanji CIty, China, July 16-20 2006.

[10] S. Kawamura and K. Ito. A new type of master robot for teleoperation using a radial wire drive system. In *Intelligent Robots and Systems '93, IROS '93. Proceedings of the 1993 IEEE/RSJ International Conference on*, volume 1, pages 55–60vol.1, 26-30 July 1993.

[11] T. Morizono, K. Kurahashi, and S. Kawamura. Realization of a virtual sports training system with parallel wire mechanism. In *Proc. IEEE International conference on Robotics and Automation*, volume 4, pages 3025–3030, Albuquerque, NM, Apr 1997.

[12] N. Tarrin, S. Coquillart, S. Hasegawa, L. Bouguila, and M. Sato. The stringed haptic workbench: a new haptic workbench solution. In *Computer Graphics Forum*, volume 22, pages 583–589. Blackwell Synergy, 2003.

[13] S. Plagenhoef. *Patterns of Human Motion: A Cinematographic Analysis*. Prentice-Hall Englewood Cliffs, NJ, 1971.

[14] RF Zernicke and EM Roberts. Lower extremity forces and torques during systematic variation of non-weight bearing motion. *Med Sci Sports*, 10(1):21–6, 1978.

[15] Y. Cai, S. Wang, M. Ishii, and M. Sato. Position Measurement Improvement on a Force Display Device Using Tensed Strings. *IEICE Transactions on Information and Systems*, 79(6):792–798, 1996.

[16] J.M. Steinacker, W. Lormes, M. Lehmann, and D. Altenburg. Training of rowers before world championships. *Med Sci Sports Exerc*, 30(7):1158–1163, 1998.

[17] L. Dovat, O. Lambercy, V. Johnson, B. Salman, S. Wong, R. Gassert, E. Burdet, T. Chee Leong, and T. Milner. A cable driven robotic system to train finger function after stroke. In *Proc. IEEE 10th International Conference on Rehabilitation Robotics*, pages 222–227, Noordwijk, The Netherlands, June 2007.

[18] S. Kim, J. J. Berkley, and M. Sato. A novel seven degree of freedom haptic device for engineering design. *Virtual Reality*, 6(4):217 – 228, August 2003.

[19] J. Albus, R. Bostelman, and N. Dagalakis. The nist robocrane. *Journal of Robotic Systems*, 10(5):709–724, 1993.

[20] S. Kawamura, H. Kino, and C. Won. High-speed manipulation by using parallel wire-driven robots. *Robotica*, 18:13–21, 2000.

[21] D.A. Lawrence, L.Y. Pao, and S. Aphanuphong. Bow spring/tendon actuation for low cost haptic interfaces. In *First Joint Eurohaptics Conference and Symposium on Haptic Interfaces for Virtual Environment and Teleoperator Systems*, pages 157–166, March 2005.

[22] E. Stump and V. Kumar. Workspaces of cable-actuated parallel manipulators. *Journal of Mechanical Design*, 128:159–167, 2006.

[23] R.L. Williams, J.S. Albus, and R.V. Bostelman. 3d cable-based cartesian metrology system. *Journal of Robotic Systems*, 21(5):237–257, 2004.

[24] S. Fang. *Design, modeling and motion control of tendon-based parallel manipulators*. VDI Fortschritt-Bericht, 2005.

[25] F. Faschinger, J. von Zitzewitz, and F. Pernkopf. Ein paralleler, 8-achsiger seilroboter mit groem arbeitsraum als handlingapplikation. In *Proc. Internationales Forum Mechatronik*, pages 218–228, Linz, Austria, 2006.

[26] E. Uhlmann, E. Schaeper, and C. Neumann. Entwicklung einer hochdynamischen skalierbaren parallelkinematik. In *3. Dresdner WZM-Fachseminar*, 2001.

[27] J-P. Merlet and D. Daney. A new design for wire-driven parallel robot. In *Proc. Design and Modelling of Mechanical Systems, 2nd world congress*, Monastir, Tunisia, 2007.

[28] T. Nef and R. Riener. ARMin - design of a novel arm rehabilitation robot. In *Proc. IEEE International Conference on Rehabilitation Robotics*, pages 57–60, 2005.

[29] S. Jezernik, G. Colombo, T. Keller, H. Frueh, and M. Morari. Robotic Orthosis Lokomat: A Rehabilitation and Research Tool. *Neuromodulation*, 6(2):108–115, 2003.

[30] K. Usher, G. Winstanley, and R. Carnie. Air vehicle simulator: an application for a cable array robot. In *Proc. IEEE International Conference on Robotics and Automation*, pages 2241–2246, Barcelona, Spain, 2005.

[31] C. Melchiorri, G. Vassura, and P. Arcara. What kind of haptic perception can we get with a one-wire interface? In *Proc. IEEE International Conference on Robotics and Automation*, volume 2, pages 1620–1625, May 1999.

[32] N. Pelechano. Real-Time Collision Detection Between Cloth And Skinned Avatars Using OBB. Technical report, Department of Computer Science, University College London, UK, 2002.

[33] D. Eberly. Dynamic Collision Detection using Oriented Bounding Boxes. *Online Paper. Magic Software, Inc*, 2007.

[34] J. von Zitzewitz, P. Wolf, V. Novakovic, M. Wellner, G. Rauter, A. Brunschweiler, and R. Riener. A real-time rowing simulator with multi-modal feedback. *Sports Technology*, in press, 2009.